Supporting Information

Size-Dependent Photoluminescence Efficiency of Silicon Nanocrystal Quantum Dots

Yixuan Yu,[†] Gang Fan,[†] Andrea Fermi,[‡] Raffaello Mazzaro,[ǂ] Vittorio Morandi,[ǂ] Paola Ceroni,[‡] Detlef-M. Smilgies,[‖] Brian A. Korgel[†*]

[†] McKetta Department of Chemical Engineering, Texas Materials Institute and Center for Nano- and Molecular Science and Technology, The University of Texas at Austin, Austin, TX, 78712-1062, United States.

[‡] Department of Chemistry "G. Ciamician", University of Bologna, Via Selmi 2, 40126 Bologna, Italy.

[ǂ] Institute for Microelectronics and Microsystems (IMM) Section of Bologna, National Research Council (CNR), Via Gobetti 101, 40129 Bologna, Italy.

[‖] Cornell High Energy Synchrotron Source (CHESS), Cornell University, Ithaca, NY 14853, United States.

*Corresponding author: korgel@che.utexas.edu

Additional Data

Average diameter and polydispersity. The average nanocrystal size and size distribution for each sample was determined from transmission electron microscopy (TEM) images and small angle X-ray scattering (SAXS) of solvent-dispersed nanocrystals. Histograms of the diameter of the nanocrystals determined from TEM images are shown in Figure S1. The histograms in Figures S1a-S1f correspond to the samples shown in the TEM images in Figures 1a-1f, respectivevly. SAXS data for the different samples are shown in Figure S2. Figure 2 shows these data replotted as Porod plots. The data are plotted as red circles and the black curves represent the best fits of the scattering profile expected for a collection of non-interacting spheres with a Gaussian size distribution.[1] For all of the samples, the polydispersity determined from the TEM images is less than what is determined by small angle X-ray scattering (SAXS). This is due to the limited sampling of nanocrystals in the TEM images compared to the SAXS measurements. SAXS provides a statistically more accurate measure of the nanocrystal size distribution. SAXS is also very sensitive to larger particles in the sample, whereas in TEM images these nanocrystals are often overlooked because they are few in number.

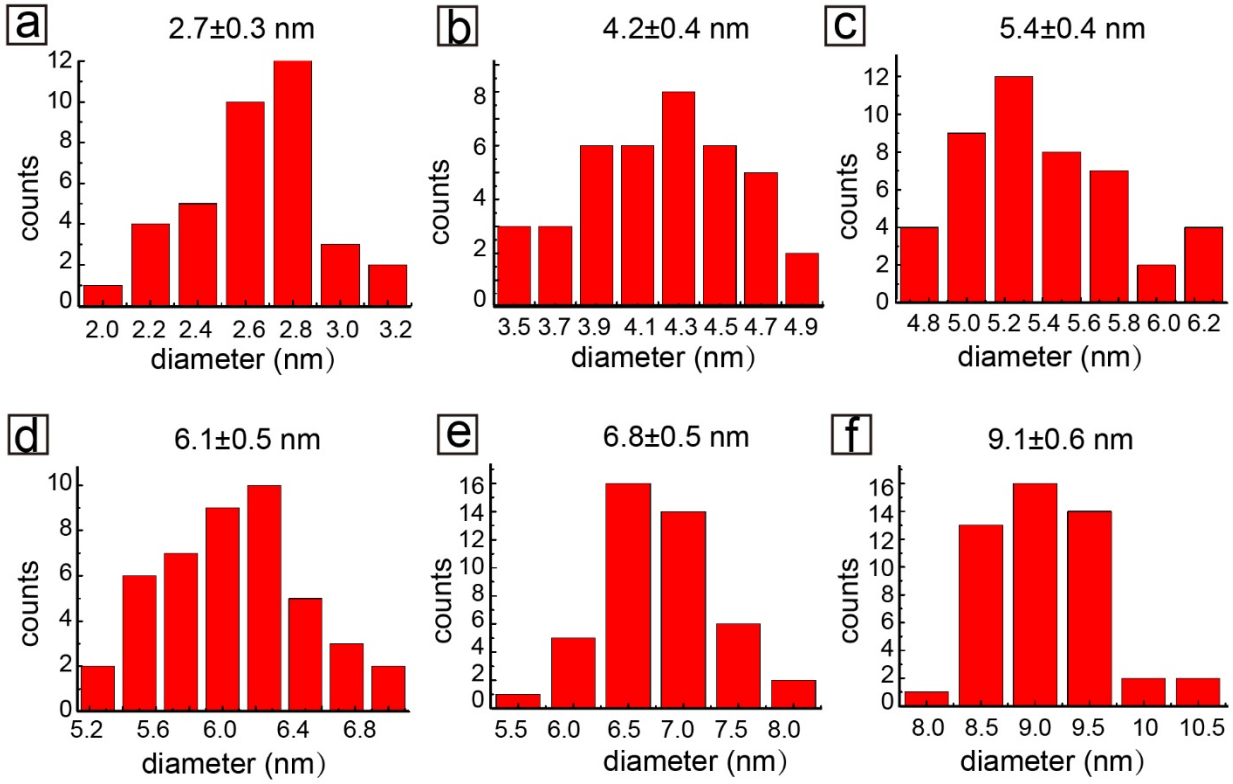

Figure S1. Histograms of the diameter of Si nanocrystals determined by TEM. The samples in (a)-(f) correspond to the nanocrystals in the TEM images in Figures 1a-1f.

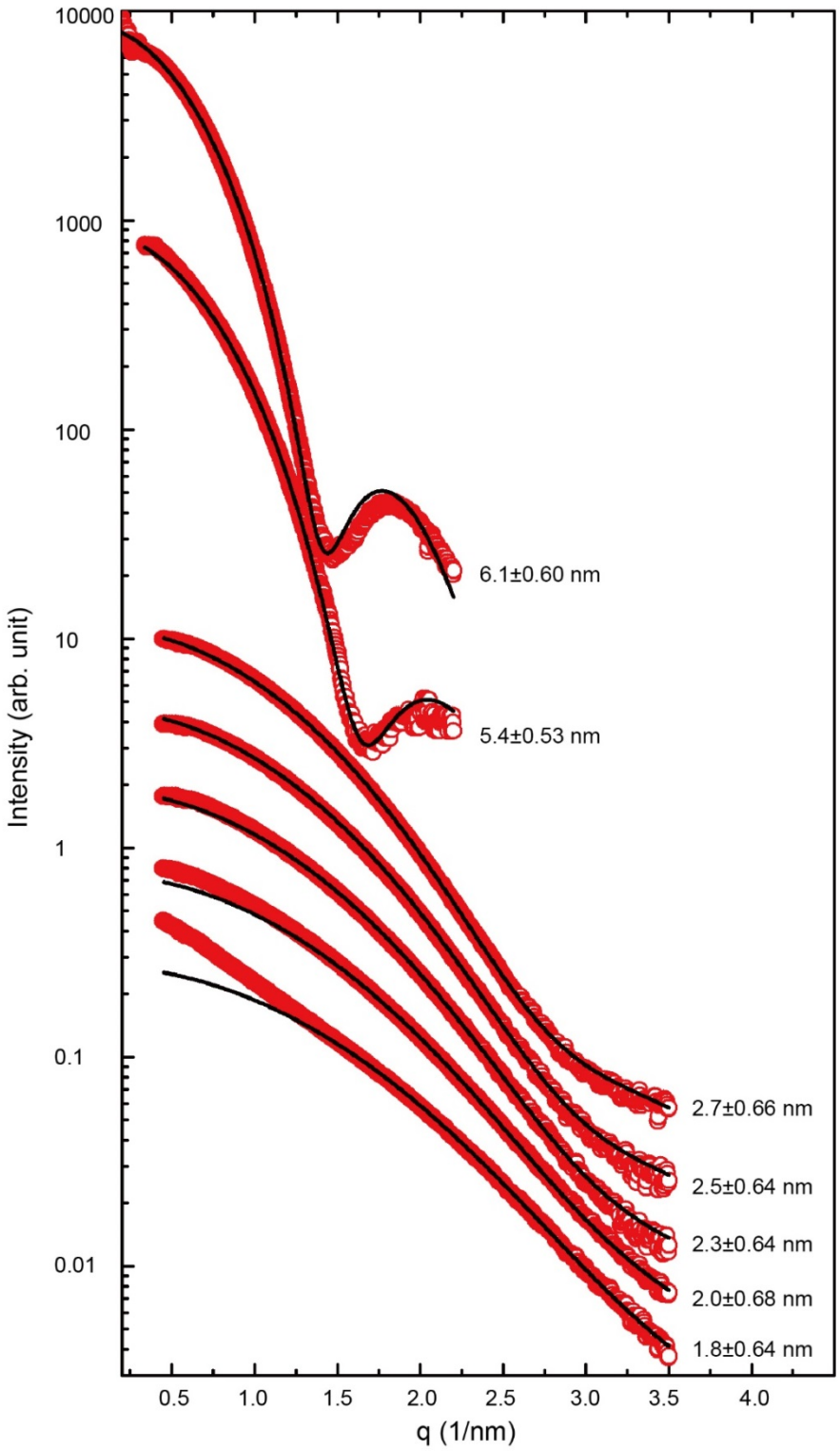

Figure S2. Small angle X-ray scattering (SAXS) data. The scattered X-ray intensity is plotted against q, the scattering wave vector, $q = (4\pi/\lambda)\sin(\theta/2)$, where λ is the X-ray wavelength and θ is the scattering angle. These data are replotted as Porod plots in Figure 2.

Fourier transform Infrared (FTIR) data. Figure S3 shows FTIR data for 3 and 5 nm Si nanocrystals, showing C-H stretching, Si-H stretching, C-H deformation, and Si-O stretching signals.

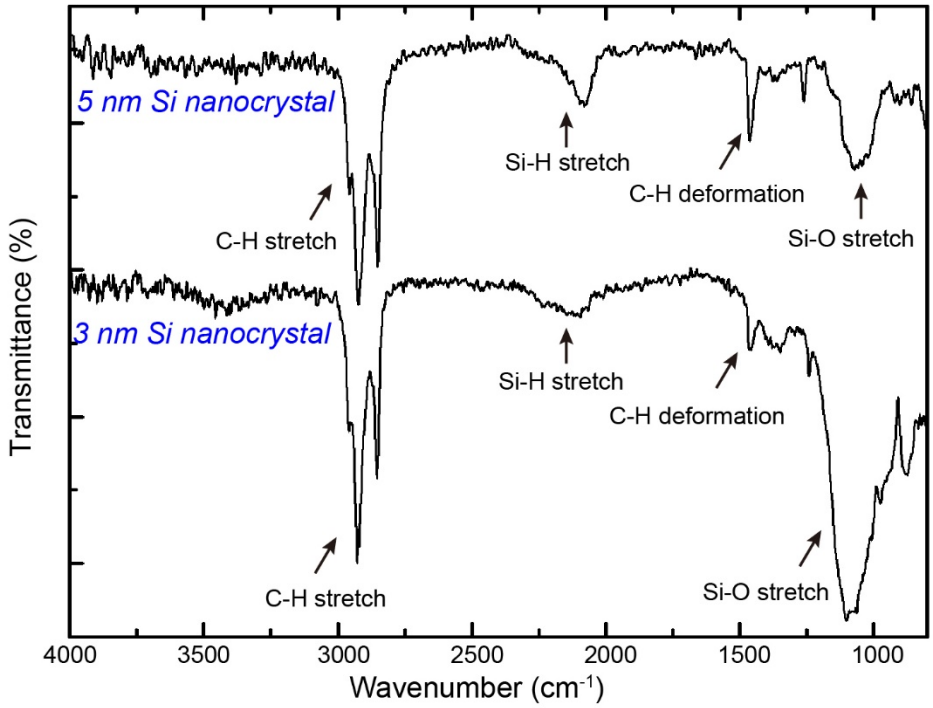

Figure S3. FTIR data for 3 and 5 nm Si nanocrystals.

Solving Schrödinger equation for the finite confinement model. The trial wave function is

$$\Psi(r_e, r_h, r_{e-h}) = A\phi_e(r_e)\phi_e(r_e)\, e^{(-r_{e-h}/\alpha)} \text{ where } \phi_i(r_i) = \begin{cases} \sin(\beta_i r_i)/r_i, r_i \le R \\ B_i\, e^{(-\xi_i r_i)}/r_i, r_i > R \end{cases}, i = e, h.$$

There are 7 variables in the wave function: $B_e, B_h, \xi_e, \xi_h, \beta_e, \beta_h, A$. B_e, B_h, ξ_e, ξ_h can be expressed as functions of β_e, β_h based on the smoothness of the wave function at the nanocrystal boundary ($r = R$); A can also be written as a function of β_e, β_h according to the normalization of the wave function over space. Therefore, the wave function finally contains two variables: β_e, β_h, which need to be determined by finding the lowest expected value for confinement energy (the ground state energy):[2]

$$E(\beta_e, \beta_h) = \int_0^\infty dr_e \int_0^\infty dr_h \int_{|r_e - r_h|}^{r_e + r_h} dr_{e-h} r_e * r_h * r_{e-h} * \Psi * H * \Psi$$

The lowest expectation of confinement energy is found numerically (Figure S4a), from which β_e, β_h, and the finite confinement energy could be determined. In the meantime, the expectation of confinement energy at $\beta_e = \beta_h = \pi/R$ should return to the value predicted by the infinite confinement model,[3] which can be used as a check point to verify the correctness of equation derivation. It is worthwhile to note that we have treated electron-hole Coulomb interaction perturbatively during the solution of the Schrödinger equation, and several expressions containing α (due to the electron-hole Coulomb interaction) with an order higher than one are neglected for the sake of simplicity.

The expression for the expectation of confinement energy is $E(\beta_e, \beta_h) = E_1 + E_2 + E_3 + E_4$, in which

$$E_1 = \frac{4}{\pi^2}\left(0.147{\beta_e}^2 + 0.106{\beta_h}^2\right)[0.5\beta_e R - 0.25\sin(2\beta_e R)][0.5\beta_h R - 0.25\sin(2\beta_h R)]$$

$$E_2 = \frac{2}{\pi^2}\left(0.147{\beta_e}^2[\frac{\cos(\beta_e R)}{\sin(\beta_e R)}]^2 - 0.106{\beta_h}^2 - 1.7\right)\frac{\sin(\beta_e R)^3}{\cos(\beta_e R)}[0.5\beta_h R - 0.25\sin(2\beta_h R)]$$

$$E_3 = \frac{2}{\pi^2}\left(-0.147{\beta_e}^2 + 0.106{\beta_h}^2[\frac{\cos(\beta_h R)}{\sin(\beta_h R)}]^2 - 1.7\right)[0.5\beta_e R - 0.25\sin(2\beta_e R)]\frac{\sin(\beta_h R)^3}{\cos(\beta_h R)}$$

$$E_4 = \frac{1}{\pi^2}\left(-0.147{\beta_e}^2\left[\frac{\cos(\beta_e R)}{\sin(\beta_e R)}\right]^2 + 0.106{\beta_h}^2\left[\frac{\cos(\beta_h R)}{\sin(\beta_h R)}\right]^2 + 3.4\right)\frac{\sin(\beta_e R)^3}{\cos(\beta_e R)}\frac{\sin(\beta_h R)^3}{\cos(\beta_h R)}$$

Figure S4a shows the confinement energy expectations for a 2 nm diameter Si nanocrystal ($R = 1\,nm$). Figure S4b shows the PL emission energy (bulk band gap plus confinement energy) predicted by the infinite confinement and finite confinement models for Si nanocrystals with no size polydispersity.

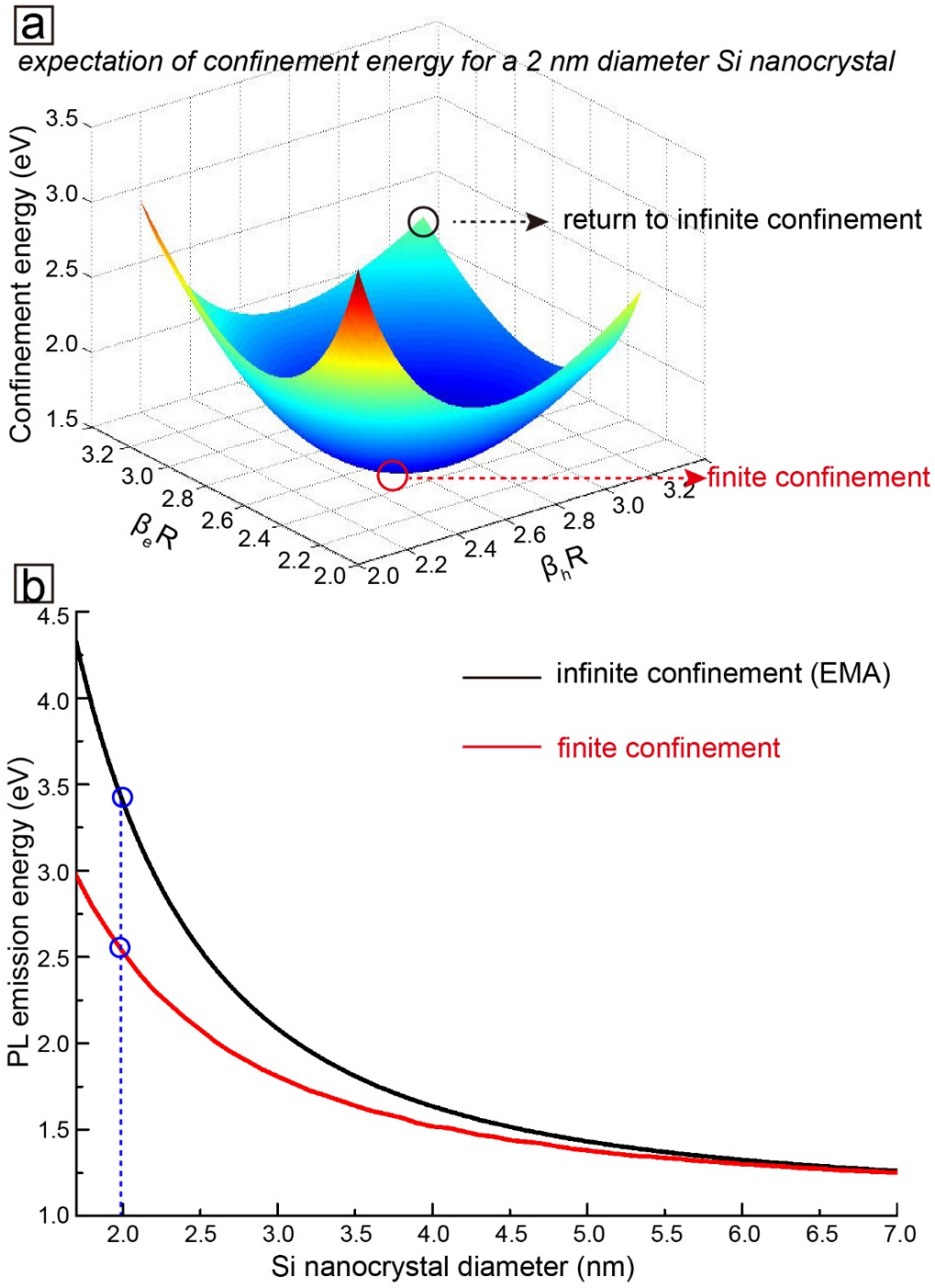

Figure S4. (a) Expectations of confinement energy of a 2 nm diameter Si nanocrystal when $\beta_e R$ and $\beta_h R$ are varied between $\pi/2$ and π; (b) predictions of PL emission energy made by infinite confinement (black curve) and finite confinement models (red curve) for Si nanocrystals (with no size polydispersity).

Figure S5 and S6 shows PLexcitation / absotption spectra for 2.5 nm Si nanocrystals and PL decay for 8.5 nm Si nanocrystals, respectively.

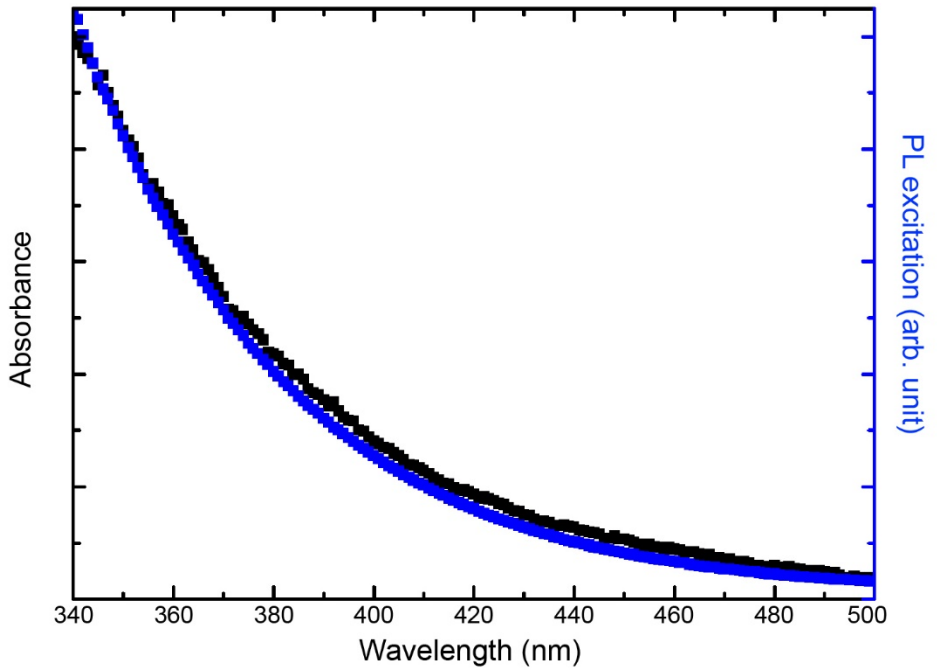

Figure S5. PL excitation and absorption spectra of 2.5 nm Si nanocrystals

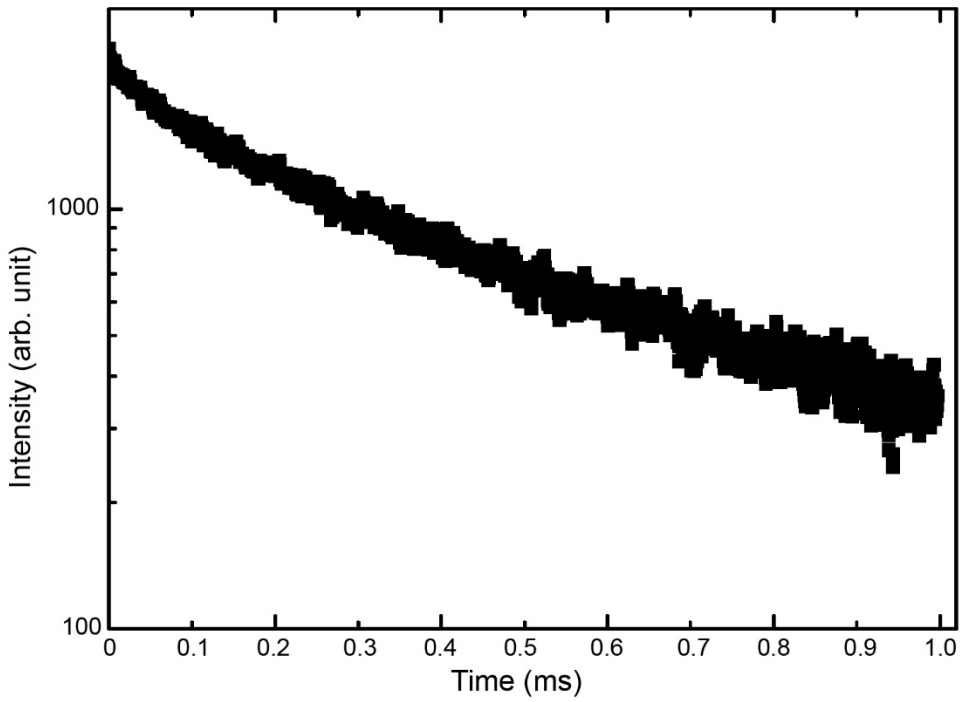

Figure S6. PL decay for 8.5 nm Si nanocrystals.

References

(1) Korgel, B. A.; Fullam, S.; Connolly, S.; Fitzmaurice, D. Assembly and Self-Organization of Silver Nanocrystal Superlattices: Ordered "Soft Spheres." *J. Phys. Chem. B* **1998**, *102*, 8379-8388.
(2) Kayanuma, Y.; Momiji, H.; Incomplete Confinement of Electrons and Holes in Microcrystals. *Phys. Rev. B* **1990**, *41*, 10261-10263.
(3) Kayanuma, Y. Wannier Exciton in Microcrystals. *Solid State Commun.***1986**, *59*,405-408.